Surface of Venus: Evidence of Diverse Landforms from Radar Observations

Abstract. *Recent radar images of the surface of Venus reveal a complex and varied terrain. By applying a set of simplifying assumptions about the nature of the surfaces returning the radar signal, it is possible to make a number of plausible interpretations. In one region on Venus, several circular features have the gross morphology of degraded impact craters. If they are indeed of impact origin, these features suggest that there exist on Venus areas which are ancient and where erosion or resurfacing has not been as intense or as pervasive as on the earth. In other regions there are intriguing features that may evidence active internal processes. One is a large trough-like depression (0°,76°W; measuring 1400 by 150 by 2 kilometers) planimetrically suggestive of both the Valles Marineris on Mars and the East African Rift on the earth. Another feature, about 250 kilometers in diameter and of positive relief, includes an 80-kilometer-diameter circular depression at its summit, suggestive of a large volcanic construct. A third region, near 0°,10°E, contains roughly parallel ranges of mountains separated by valley-like features, with relief varying from small isolated hills several hundred meters high to low ranges on the order of 1000 meters to large mountains approaching 2 kilometers in height. If Venus has a mobile crust similar to the earth's, these mountains may have been produced by compressional tectonics. These interpretations of the radar data indicate that Venus has been a geologically active planet which has developed diverse landforms and therefore is an exciting candidate for future exploration.*

For many years the planet Venus was considered to be the earth's twin: similar densities, sizes, and position in the solar system were the dominant reasons for this point of view. The obscuration of surface features by a cloudy atmosphere and the lack of detail within the clouds did little to dispel the twin planet concept. Only after earth-based and spacecraft measurements of temperature and pressure indicated an intensely hot, massive carbon dioxide atmosphere did Venus begin to take on an individual character. Current discussions of exotic atmospheric species such as sulfuric acid are indicative of the shift in point of view. Without observations of the surface, however, the twin planet idea, especially as it might be related to the tectonic and volcanic evolution of the planet, cannot be evaluated.

While the venusian atmosphere is essentially opaque at visible and infrared wavelengths, it is optically thin at centimeter wavelengths. Thus radio telescopes that can transmit as well as receive can probe the surface through the atmosphere.

The first moderately high resolution (~ 10 km per element) radar image of Venus showed several features suggestive of craters (*1*). In this report, new radar data acquired at the Jet Propulsion Laboratory's Goldstone station (*2–8*) will be discussed within a framework of interplanetary comparison of morphologic features. Speculative interpretations will be presented based on a set of assumptions regarding radar reflective properties of the surface of Venus.

Three variables affect the radar return from a planetary surface at both local and regional scales: slopes, surface roughness, and the dielectric properties of the surface materials. For areas far from the subradar point (that is, the center of illumination) slopes probably play a smaller role, while for areas closer to the subradar point they may play a more important role. For the interpretation of the radar images used in this study, the following simplifications were made.

1) The imaged regions are circular caps on the front of the planet with radii of a little more than 6 planetocentric degrees (about 650 km) around the subradar point. The apparent source of illumination is at the center of each image. Areas of greatest radar return (the brightest areas on the image) are those whose surface elements (either local slopes or facets of debris and blocky rubble) are oriented normal to the line of illumination from the antenna to the point of surface return (*9*).

2) In the absence of large-scale geometric effects, reflectivity is more dependent on variations in surface roughness on the order of the wavelength of the radar than it is on the dielectric properties of a reasonable suite of silicate materials. Thus, radar "albedo" variations that cannot be attributed to slopes are attributed to surface roughness.

Observations. Discussion of the initial high-resolution radar image has emphasized the readily apparent circular features and interpreted these as craters of unknown origin (*1*). Subsequent work on the images (*2, 10, 11*) has suggested impact as the primary mode of formation. Although several circular features have been observed, their unambiguous interpretation as depressions with raised rims has not been established. A few have rims (as evidenced by radar photometric shading) but do not appear as depressions on altimetry maps, even though they are many resolution elements across. Others appear depressed but without bounding rims. Preliminary size-frequency and morphology studies (*10, 11*) of features tentatively identified as craters show trends similar to those observed for degraded lunar and martian craters. This is not conclusive evidence of an impact origin for these features on Venus, but it is suggestive.

The most startling feature yet seen on Venus is shown in Fig. 1. These mosaics of two reflectivity (top) and altimetry (bottom) images show a large, trough-like feature 1400 km long, 150 km wide, and approximately 2 km deep. The northern portion of the trough consists of several north-trending lineaments, two of which form opposing scarps with scalloped walls suggesting a crater chain. To the south, the trough divides in two. Each of the subtroughs is some 100 km across. None of the branches terminate within the radar field of view, suggesting that the trough system may be more than 1400 km long. A ridge or septum appears to run the length of the linear portion of the trough system, which accounts for the trough's elevated interior as seen in the lower-resolution altimetry data. The rim of the trough appears to be raised on the altimetry map. Since the altimetry is referenced to a locally spherical planet, the raised rim suggests a marked deviation from sphericity, probably in the form of regional doming.

To the east and west of the trough are essentially featureless "plains" regions of moderately high radar reflectivity. This suggests that the surface is relatively rough on the order of the radar wavelength ($\lambda \cong 12.6$ cm). Individually restricted areas of prominent reflectivity difference correlate well with isolated topographic features seen on altimetry maps. East of the plains, an elevated region of high radar contrasts, bounded by a sharp escarpment, rises some 1 to 1.5 km. The extremely variable return of this plateau suggests a rough and complex topography. Within the plateau several smaller, more elevated spots show high reflectivity on their earthward-facing slopes, which suggests that they are isolated mountains.

Figure 2 shows a slightly elevated, elliptical region approximately 800 km long and 450 km wide centered near 10°S, 40°W. Atop this broad rise is a more sharply defined, domical feature about

250 to 300 km across and 1 km high. The summit is occupied by a "crater" 60 to 90 km in diameter with precipitous inner slopes and gentle outer slopes. Its southern wall appears multiply scarped. A major ridge, in places exceeding in elevation the crater rim, extends more than 200 km east from the crater. A small, subsidiary crater (~ 30 km across) is barely resolved immediately north and east of the large crater, on the smooth, shallow slopes near the summit of the domical structure. The ratio of rim width to floor diameter of the large crater is similar to those of both martian and terrestrial volcanic calderas (*10*).

A region centered near 9°S,10°E contains a cluster of small (≲ 60 km) individual peaks that appear to form roughly arcuate ranges (Fig. 3). The region is somewhat less than 1 km higher than the surrounding plain, which appears moderately smooth on the order of the radar wavelength (≅ 12.6 cm). Approximately 15 peaks can be resolved, all of which are confined to an area of less than 300 km square.

Also seen in Fig. 3 is a region of roughly parallel ranges of hills and valleys, with major axes east-west, located near the venusian equator at 10°E. Traversing north across the ranges from the plains immediately south of the region, the topography varies from a few hundred meters to 1 to 2 km of local relief. A few closed circular depressions are seen within the area of rough terrain. The boundary between the plains and the hills and valleys is sharp and linear, with shading suggestive of a pronounced scarp. Several lineaments intersect the boundary, including one trending north-northeast to south-southwest near 4°S,8°E.

Finally, an arcuate ridge more than 800 km long but less than 30 km across is shown in Fig. 4 at 2°S,8°W. Available altimetry does not resolve the ridge, although the region bounded by the arc appears somewhat depressed relative to the surrounding surface. A lineament crosses the arc at a right angle at 2°S,7°W, causing an appreciable inward "bowing" of the ridge.

Interpretations. There exist on Venus roughly circular forms that display rim width/floor diameter ratios and size-frequency relationships similar to those of large degraded craters on the other solid planets and the moon. It is reasonable to postulate that these are indeed large impact craters and therefore the regions they occupy are ancient (the abundance of large craters implies great age) (*10*, *11*). This implies that erosion on Venus in these areas has not demonstrably exceeded the cumulative total of that on cratered regions of Mars and that the resurfacing of Venus has not been as complete as that of the earth, where no ancient cratered surfaces survive. As on the moon, Mars, and Mercury, there are regions of Venus that have retained these ancient features and regions that have been modified. We postulate that combined effects of tectonism and volcanism produce this selective resurfacing on Venus. Within this framework, the other landforms on Venus provide some insight into these processes.

The planimetric and topographic configuration of the venusian trough system (Fig. 1) is strikingly similar to that of the Valles Marineris trough system on Mars (*12*), which in turn has been extensively compared with terrestrial features such as the East African Rift system (*13*, *14*). The East African Rift system consists of both regions of incipient crustal spreading and regions of upwarp and graben formation through extension of the crust (*15*). The Valles Marineris has been interpreted as suggesting either subsidence or crustal extension, with subsequent exogenous erosional modification. Whether the venusian trough system has associated spreading phenomena cannot be determined from images with 20-km resolu-

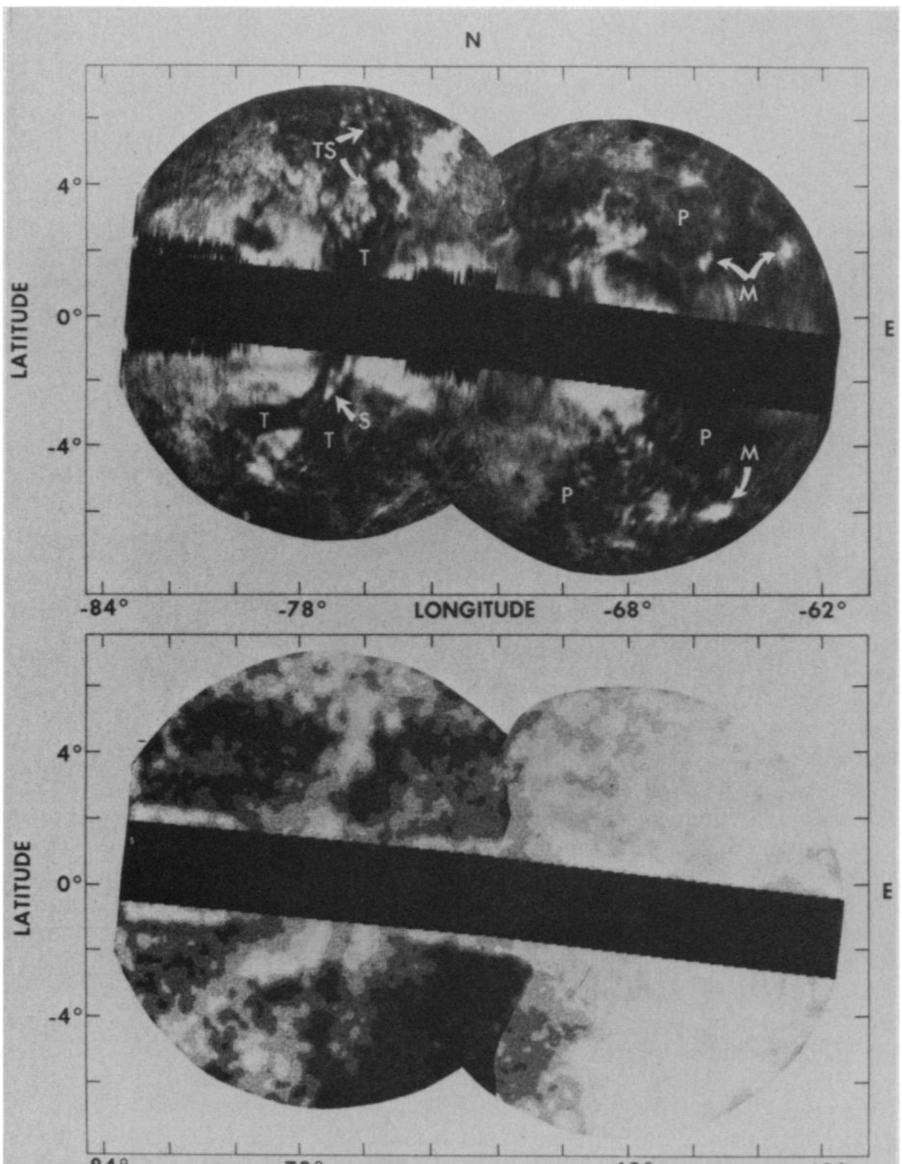

Fig. 1. Radar observations of Venus. (Top) This mosaic of two radar reflectivity images is based on data acquired by Goldstein and co-workers at the Goldstone Tracking Station (*2*). The area is ~ 2300 × 1400 km². Note the large, trough-like feature in the left image (*T*) and the mottled plateau in the right (*P*). Important features of the trough include a region with scalloped walls suggestive of a crater chain (*TS*), a ridge or septum running the length of the more linear reach of the trough (*S*), and a bifurcation near 4°S,78°W. Within the plateau, several isolated peaks can be seen (*M*). The image resolution is about 20 km. The trough is interpreted as evidence of extensional tectonic activity on Venus. (Bottom) Altimetry map of trough and plateau region on Venus. The contour interval is ~ 400 m, the resolution is ~ 50 to 60 km.

tion. It seems possible, however, that the feature does indicate the existence of extensional tectonic activity on Venus.

The large (> 400 km) domical form with the summit crater is reminiscent of the Tharsis volcanoes on Mars (*16*), although the topography is far less dramatic. The Tharsis volcanoes have been discussed in terms of a mantle source providing material to penetrate an essentially motionless lithosphere, with the great height of the volcanoes related to the thickness of the lithosphere (*16, 17*). Combined with the greater abundance of craters of possible impact origin within this region, the observation of a Tharsis-type volcano might suggest a similarly stable crust, albeit of somewhat less thickness or lower strength (perhaps because of higher interior temperatures).

The cluster of peaks seen in Fig. 3 is unusual in that such occurrences are rarely seen on Mars, Mercury, or the moon. Such features are more common on the earth, however, associated with centers of concentrated volcanic activity such as the San Francisco Peaks region in Arizona (*18*) or the Tibesti Volcanic Province in Chad, Africa (*19*). A similar origin of the landform seen in the Venus radar data would suggest a second type of volcanism (that is, one that forms clusters of relatively small peaks rather than a single large construct).

The region of hills and valleys, and the lineaments associated with the boundary of the region, suggest tectonic activity. However, several alternative interpretations are consistent with the observations. One interpretation suggests that the mountains and valleys are of compressional origin, like the European Alps or Tibetan Himalayas (*20*). An alternative is that they result from extension of the type that formed the basin-and-range topography seen in the western United States (*21*). The lineaments probably reflect tectonic processes as well, and are interpreted as fault zones, although the exact nature of motion (thrust, high-angle reverse, or lateral) is not discernible in

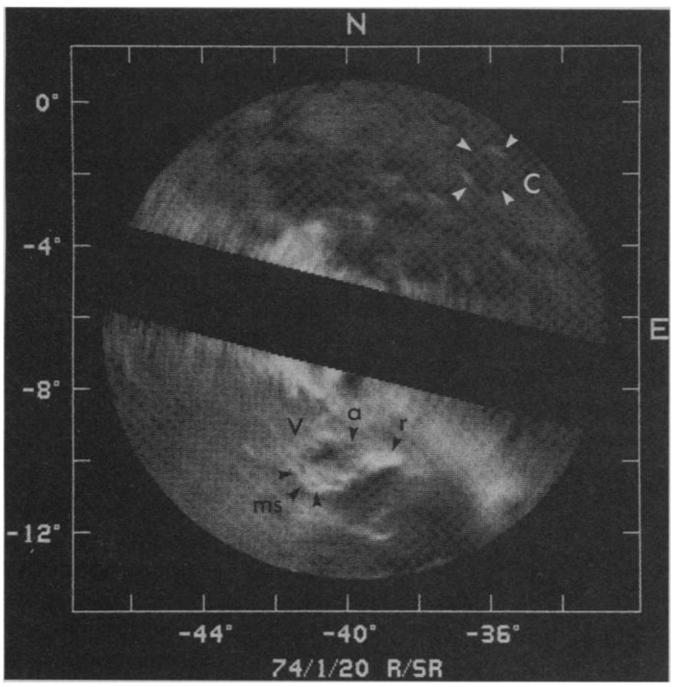

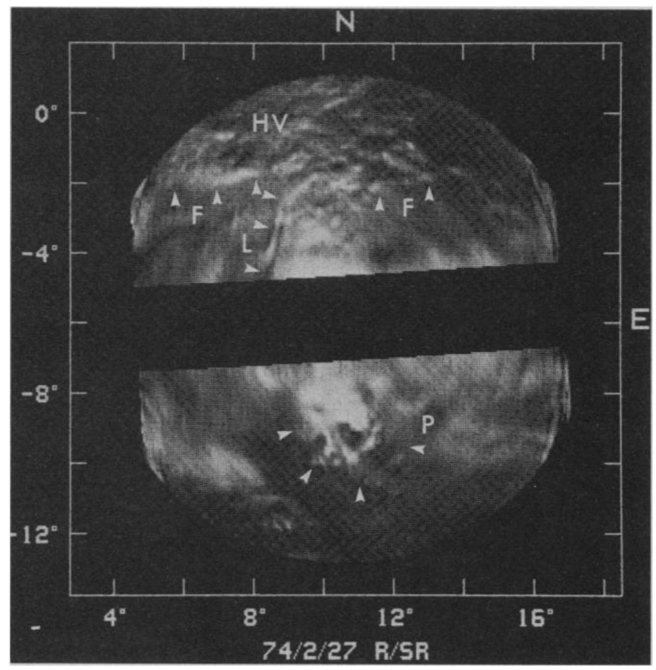

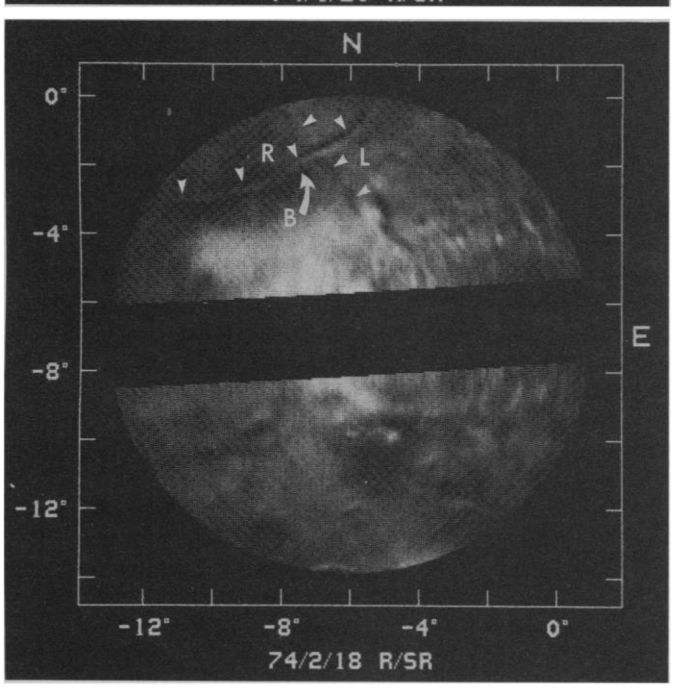

Fig. 2 (upper left). Reflectivity image of Venus: single radar image taken at the Goldstone Tracking Station. Highlighted light and dark features are topographic slopes. Goldstein and co-workers (*2*) and Saunders and Malin (*10*) identify *C* as a crater-like form. Feature *V* is interpreted here as a volcanic construct similar to the Tharsis volcanoes on Mars. Note the large ridge extending to the east of the central crater (*r*), the multiply scarped rim (*ms*), and the satellitic crater (*a*). The lettering at the bottom indicates the date of observation (20 January 1974) and that the image brightness represents the actual radar reflectivity at any point (*R*) divided by the square root of the average power dependence on angle of incidence, the backscatter function (*SR*). The latter correction preserves for cosmetic purposes some shading related to the planetary curvature. The image is about 1400 km across. Fig. 3 (upper right). Radar reflectivity photograph of Venus: single radar image taken on 27 February 1974. Note the cluster of peaks isolated on a smooth plain (low radar reflectivity) (*P*). Note also the ranges of hills and valleys near the equator (*HV*). Strong linear trends representing the front of the hill and valley terrain (*F*) and a dramatic lineament that intersects the front (*L*) are interpreted as fault zones. The image is about 1400 km from top to bottom. The cluster is interpreted as a group of volcanic peaks, and the hills, valleys, and lineaments as evidence of either compressional or extensional tectonism. Fig. 4 (lower left). Radar image of Venus. This single radar frame shows an area about 1400 km in diameter. The most conspicuous feature is the 800-km-long arcuate ridge (*R*) in the upper portion of the image. Note the lineament (*L*) which seems to displace, or bow, the arc inward (*B*). The nature and origin of the arc are unclear, but the lineament is interpreted as a fault zone with some right-lateral motion.

the radar images. Thus, in contrast to other regions on Venus, where craters seem to imply a quiescent surface history, this portion of the planet appears to have experienced tectonic modification at least as severe as that seen on Mars, and perhaps similar to that associated with terrestrial plate tectonic activity.

Summary. The recent radar images of Venus suggest the following features and interpretations.

1) Circular features in some areas may be of impact origin. If so, their existence implies relatively quiescent surface modification processes.

2) A great trough-like depression near 0°,76°W suggests extensional tectonic activity.

3) Two types of central volcanism (one forming single large constructs and one forming clusters of smaller peaks) are suggested by the interpretation of features near 10°S,40°W and 10°S,10°E.

4) A region of mountainous terrain and sharply defined lineaments may indicate compressional tectonism, although extension could also explain these features.

5) Large expanses of moderate or high reflectivity suggest bouldery surfaces, a point well illustrated by images of the surface of Venus returned by the Soviet spacecraft Venera 9 and Venera 10.

In conclusion, the radar images in part seem to indicate that some regions of Venus have remained little altered since a period of intense bombardment similar to that recorded by the many large impact craters on the moon, Mercury, and Mars. On the other hand, there is evidence in other regions that Venus has been a geologically active planet, forming diverse landforms, and perhaps rivaling the earth in the breadth of features portrayed on its surface. The possibility of studying features remarkably like those on the earth make Venus an exciting candidate for future exploration.

MICHAEL C. MALIN
R. STEPHEN SAUNDERS
Planetology and Oceanography Section, Jet Propulsion Laboratory, California Institute of Technology, Pasadena 91103

References and Notes

1. H. C. Rumsey, G. A. Morris, R. R. Green, R. M. Goldstein, *Icarus* **22**, 1 (1974).
2. R. M. Goldstein, *Eos* **56**, 388 (1975); ___, R. R. Green, H. Rumsey, *J. Geophys. Res.* **81**, 4807 (1976).
3. On 23 and 28 December 1973, 13 and 20 January 1974, and 1, 18, and 27 February 1974, Venus was observed by using the Goldstone 64-m antenna to transmit a 400-kw, continuous-wave, 12.6-cm signal, and both the 64-m and a 26-m antenna to receive the echoes (*1, 2*). The interferometer baseline was 22 km. Each Doppler–time delay cell was approximately 10 km square. A brief discussion of the radar technique used to acquire the data shown here is presented in (*4*).
4. The radar techniques used to produce the images discussed here analyze the returned echo in time, frequency, and power. In the application of these techniques, the reflected signals are "chopped" in time slices as they are received, forming collar-like zones concentric with the subradar point [see figure 1 in (*5*) and figure 2, a and b, in (*6*)]. The more rapidly the signal is sampled, the smaller the width and the higher the resolution. These zones are generally called time delay or range gates. Frequency analyses of the range-gated echoes, which capitalize on Doppler shifts associated with planetary rotation, provide a second spatial coordinate. Lines of equal Doppler shift (both positive and negative) are circles parallel to the plane containing the rotation axis and the subradar point and are thus seen edge-on by the radar as lines parallel to the rotation axis. Again, the finer the frequency slices, the higher the resolution. High resolution is inhibited, however, by the fact that time delay and frequency slices must be weighed against the integration time and area required to achieve a reasonable signal-to-noise ratio for the returned echoes. Three problems arise from these observational techniques. (i) A given pair of time-delayed and Doppler-shifted values can be mapped to two locations symmetrically above and below the radar equator defined by the plane perpendicular to the rotation axis and containing the subradar point [see figure 2 in (*6*)]. This north-south ambiguity can be eliminated by two techniques. The first is a form of single-antenna "stereo" viewing and multiple-antenna "interferometry." The apparent stereo angle is acquired over many days as the subradar point moves across the surface of Venus in response to terrestrial and venusian rotational and orbital motions. By viewing the echoes from multiple "positions," and watching for variations in the signal strength of individual cell returns as the subradar point moves north or south, it is possible to remove most of the major effects of the ambiguity (*5, 7*). In the second technique two signals (received by two antennas used as an interferometer), which are shifted in phase because of the separation of the antennas, are combined to produce contours of constant phase shift. These contours can be used to alleviate the north-south ambiguity, since the two cells with the same Doppler and time delay have phases of opposite sign (*1, 8*). (ii) The so-called poison points (*1*) result when, because of insufficient rotation of the interferometer baseline, it is not possible to distinguish null points of integer phase, which are seen most prominently in the altimetry maps as bands parallel to the radar equator. (iii) Finally, because the time delay and Doppler coordinates are parallel at, and perpendicular to, the radar equator [see figure 2 in (*6*)], and because of the large size of the front cap range ring (*1*), the data from these portions of the Venus radar images have been suppressed. Thus each image contains a black zone along the radar equator, called the runway (*1*).
5. R. M. Goldstein and H. Rumsey, *Science* **169**, 974 (1970).
6. S. Zohar and R. M. Goldstein, *Astron. J.* **79**, 85 (1974).
7. R. M. Goldstein and H. C. Rumsey, *Icarus* **17**, 699 (1972).
8. A. E. E. Rogers and R. P. Ingalls, *Radio Sci.* **5**, 425 (1970).
9. Thus, regional slopes in the direction of the subradar point having the same inclination as the radial distance in degrees will appear brightest. For example, if there were a domical hill 2° from the center of the image, that part of the hill having a local slope of 2° toward the image center would appear brightest. Conversely, the darker part of the feature would be that part with the greatest slope away from the image center. Shadows occur when the slope away from the subradar point exceeds the complement of the angular offset.
10. R. S. Saunders and M. C. Malin, *Geol. Rom.*, in press.
11. G. G. Schaber and J. M. Boyce, *Moon*, in press.
12. R. P. Sharp, *J. Geophys. Res.* **78**, 4063 (1973).
13. W. K. Hartmann, *Icarus* **19**, 550 (1973).
14. P. Masson, *ibid.* **30**, 49 (1977).
15. B. H. Baker, P. A. Mohr, L. A. J. Williams, *Geol. Soc. Am. Spec. Pap. 136* (1973).
16. M. Carr, *J. Geophys. Res.* **78**, 4049 (1973).
17. ___, in *Proceedings of an International Colloquium on Planetary Geology*, Rome, September 1975.
18. H. S. Colton, *Mus. North. Ariz. Bull. 10* (1950).
19. P. M. Vincent, in *African Magmatism and Tectonism*, T. N. Clifford and I. G. Glass, Eds. (Hafner, Darien, Conn., 1970), p. 301.
J. F. Dewey and J. M. Bird, *J. Geophys Res.* **75**, 2625 (1970).
21. L. Wright, *Geology* **4**, 489 (1976).
22. This report presents the results of one phase of research carried out at the Jet Propulsion Laboratory under contract NAS 7-100, sponsored by the Planetology Program Office, Office of Space Science, National Aeronautics and Space Administration.

28 December 1976

Photoassisted Electrolysis of Water by Visible Irradiation of a *p*-Type Gallium Phosphide Electrode

Abstract. *Photoelectrolytic decomposition of water with visible irradiation is demonstrated in a cell made of p-type gallium phosphide as the cathode and platinum as the anode. A maximum energy conversion efficiency of 0.1 percent is achieved with an external bias of 1.3 volts. The stability of the electrode is demonstrated, and the results are discussed in terms of a composite energy diagram.*

Of the various schemes to convert solar energy into chemical energy, photoassisted electrolysis of water is beginning to show promise as a practical method. Photoassisted electrolysis of water by ultraviolet irradiation of *n*-type semiconductor electrodes has been demonstrated in a number of systems (*1, 2*). The significance of a photoelectrolytic device for the conversion and storage of solar energy was emphasized in a number of publications during the last few years (*3*). Such a system must fulfill three basic requirements: (i) it must bring about the light-

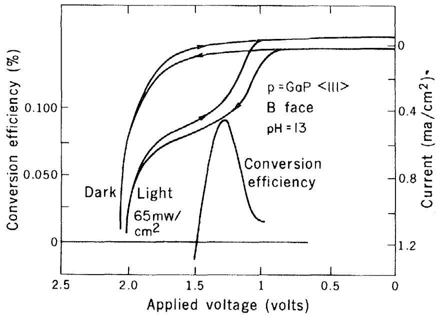

Fig. 1. Current-voltage and conversion efficiency–voltage diagrams for a cell made of Zn-doped GaP, ⟨1̄1̄1̄⟩ as the cathode and Pt foil as the anode. The electrolyte was $10^{-2}M$ NaOH + 0.5M Na_2SO_4. The light source was an attenuated, water-filtered, 75-watt Xe lamp.